EGYPTIAN DENTAL JOURNAL
VOL. 63, 509:522, JANUARY, 2017
I.S.S.N 0070-9484
ORAL MEDICINE, X-RAY, ORAL BIOLOGY AND ORAL PATHOLOGY
www.eda-egypt.org • Codex : 85/1701

EVALUATION OF THE BONE REGENERATION EFFICACY OF MAGNESIUM BIOACTIVE GLASS VERSUS ZINC BIOACTIVE GLASS BOTH LOADED WITH BONE MORPHOGENETIC PROTEIN-2 IN EXTRACTION SOCKETS OF DIABETIC ALBINO RATS

Marwa M.S. Abbass* *and* Zeinab A. Salem**

ABSTRACT

Background: Delayed wound healing is one of the major complications of diabetes. The aim of the present study was to enhance bone regeneration in extraction sockets of diabetic rats through controlled release of bone morphogenetic protein-2 (BMP-2) from 2 types of bioactive glass scaffolds

Methods: Ninety male Albino rats were utilized in this study. Diabetes was induced by 4 daily intraperitoneal injections of streptozotocin. The first right mandibular molar was extracted for all rats. The rats were randomly assigned into three groups (GI, GII and GIII) (30 rats each) according to the date of sacrifice 3,7 and 9 days after extraction. The three main groups were subdivided into: ***Control subgroup*** **(Con)**, ***Mg*** **(Mg)** and ***Zn*** **(Zn)** ***Bioactive glass subgroups.*** The bone regenerative efficacy of the scaffold materials were evaluated histologically, immunohistochemically and histomorphometrically.

Results: A significant increase in the newly formed bone area percentage has been recorded in the Zn subgroup more than the Mg subgroup within GII and GIII where (P<0.001). The immunohistochemical results revealed a significant increase in vascular endothelial growth factor (VEGF) expression within GI and GIII subgroups where (P=0.002 and P=0.001) respectively. On the other hand there was a non significant increase in VEGF expression between GII different subgroups (P=0.267).

Conclusions: Mg and Zn enriched bioactive glass mixed with BMP-2 were capable to enhance wound healing and bone formation in extraction sockets of diabetic rats. Zn bioactive glass was more effective as it enhanced angiogenesis in the healing sockets.

KEYWORDS: Mg bioactive glasses; Zn bioactive glasses; Scaffolds; Extraction sockets; Streptozotocin induced diabetic rats.

* Assistant Professor, Oral Biology Department, Faculty of Oral and Dental Medicine, Cairo University.
** Lecturer, Oral Biology Department, Faculty of Oral and Dental Medicine, Cairo University.

INTRODUCTION

Diabetes affects hundreds of millions of people in the world. Impairment in the wound healing process has been documented as one of its major complications. Multiple complex pathophysiological mechanisms are involved in this. Diabetes is associated with a situation of hypoxia, which may be derived from insufficient angiogenesis. Hypoxia can exaggerate the early inflammatory response that leads to prolonged injury by increasing the levels of reactive oxygen species (ROS). [1,2] It should be mentioned that the two actions are closely related, as oxidative stress can lead to inflammation and vice versa.

Furthermore, diabetic hyperglycemia leads to the formation of advanced glycation end products that interact with their receptors. This interaction causes the generation of more ROS that subsequently impaired the wound healing as well. [3] Diabetes is also associated with high levels of matrix metalloproteinase which leads to tissue destruction and inhibits normal repair process. [2,4]

It has been documented that the defective vasculatures in diabetic patients is greatly influenced by the decrease of vascular endothelial growth factor (VEGF) which is the primary pro-angiogenic factor in wounds. [5,6]

Tooth loss is frequently accompanied by a progressive alveolar bone resorption, a situation that triggers bone ridge atrophy and causes difficulty to the placement of conventional or implant-supported prostheses. In addition, the osseo-integrated implants can barely or not be installed at all. [7-10] Therefore, preservation of the alveolar process in areas of tooth loss and adoption of procedures that minimize bone loss or recuperate the desirable alveolar ridge dimensions are important goals in dental practice.

A variety of synthetic materials have been used to fill bone defects and stimulate osteogenesis; among them are the bioactive glasses (BG), which are silica-based, surface-active compounds with the ability to bond directly to bone and exert an osteoconductive property. [11]

Bone morphogenic protein (BMP) is known as an endogenous growth factor, binding to cell surface receptor that is likely to play a crucial role in osteoblast stimulation and resulting in bone formation. [12] BMP can be efficiently loaded and released from BG scaffolds and composites. It is obvious that BG significantly influences the loading, release of drugs and growth factors. The drug delivery by BG is not only affected by its pore structure, but also the preparation methods. [13]

Zinc (Zn) is an essential micronutrient mineral that functions as a catalytic, structural and regulatory ion necessary for many important biological processes.[14] They include growth, development, neurological regulations, immune function and transcription processes. [15] It has been reported that zinc could work as an anti-inflammatory molecule, antioxidant molecule, or both. [16]

Magnesium (Mg) plays an important role in blood pressure regulation by modulating vascular tone and reactivity. In vitro studies have demonstrated that magnesium acts as a calcium channel antagonist [17,18] and it has also been shown to stimulate prostacyclin production.[19,20]

The purpose of the present study was to compare the healing potential of bioactive glass enriched with magnesium versus that enriched with zinc both loaded with BMP-2 in extraction sockets of diabetic Albino rats.

MATERIALS AND METHODS

Material preparation

82 ml of Tetraethyl orthosilicate (TEOS) was hydrolyzed in 500 ml distilled water and 500 ml ethanol for 1h at room temperature at pH 2. Addition of 52.5g of Ca nitrate on the above mentioned solution with continuous stirring was performed for 30 min. In order to prepare two nano-bioactive glass scaffolds incorporated with Mg or Zn,

a 95.44 g of Mg(NO3)2.6H2O) or a 54.81g of (Zn (NO3)2.6H2O) was added to the above mixture with continuous stirring for 30 min (A). Dissolving of 4.25 g of ammonium dihydrogen phosphate in 400 ml of distilled water was performed (B). Titration of B on A with continuous stirring overnight was held. Both materials were dried at 80°C for 2-3 days and fired at 600 °C for 3 h. The Oxide composition (weight %) of Magnesium bioactive glass (Mg BG) and Zinc bioactive glass (Zn BG) was CaO: 35; P2O5: 5;SiO2: 45. However Mgo: 15 (for Mg BG) and ZnO: 15 (for Zn BG).

Scanning electron microscope (SEM) (Quanta Field Emission Gun 250, FEI Company, USA), attached to an EDX Unit, with an accelerating voltage of 200 V- 30 K.V was used to investigate the morphology of the nano particles. The Mg bioactive glass powder had an average particle size of 29±3 nm while the Zn bioactive glass powder had an average particle size of 13±3 nm (Fig.1).

Experimental animal:

Ninety male Albino rats ranging from 150-200 gm were utilized in this study. The animals were housed in separate cages in a room with a 12-h day–night cycle, temperature of 24 ± 2ºC and relative humidity of 70-80%. All animals were fed with standard pellets diet and tap water ad libitum for 10 days before the start of the experiment. The experimental protocol was reviewed and approved by the Ethics Committee of the Faculty of Dentistry, Cairo University, Egypt.

Induction of diabetes and assessment of hyperglycemia

Diabetes was induced by 4 daily intraperitoneal injections of Streptozotocin (STZ) (35 mg/kg; TOKU-E Ltd. company, Bellingham, WA, USA) diluted into 2 ml of sterile citrate buffer (pH 4.5). Additional control mice were used and injected with citrate buffer alone. Daily monitoring of blood glucose levels was performed for all rats using Freestyle glucose meter (Abbott Laboratories, Illinois USA), until the end of the experiment. Animals whose blood glucose level exceeded 200 mg/dl were considered diabetic. Furthermore, non-fasted whole blood (0.05 mL) was collected from the tail vein, seven days after the first injection of either streptozotocin or citrate buffer. Plasma was separated and the glucose level was assessed using glucose oxidase method (Sigma). This was repeated 3 days later to ensure that all the rats had became diabetic.

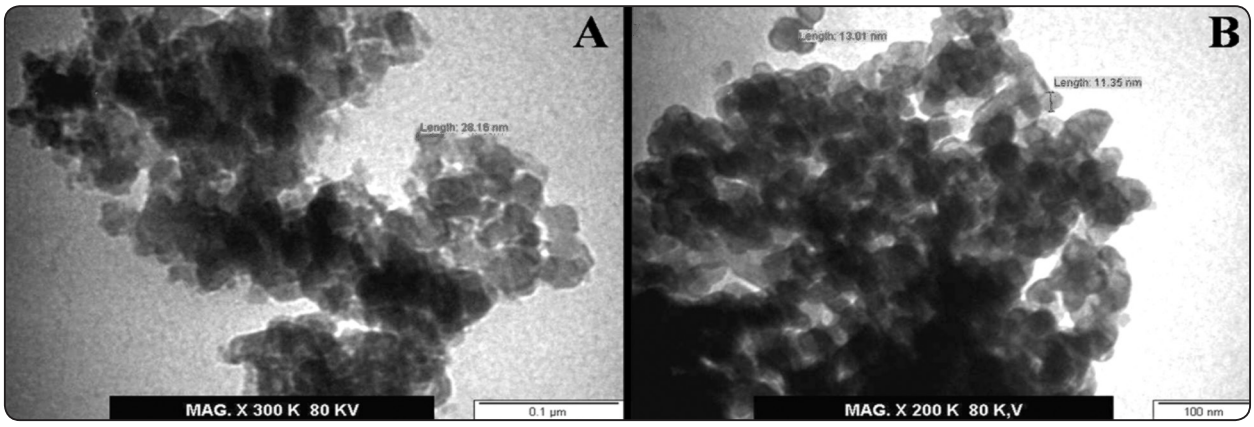

Fig. (1) SEM micrograph showing the nanostructure of Mg bioactive glass [A] and Zn bioactive glass [B].2.2. Animals

Teeth extraction

For all rats the first right mandibular molar was extracted under general anesthesia induced by intraperitoneal injection of Xylazine hydrochloride (2 mg/kg) and Ketamine hydrochloride (20 mg/kg). Extraction was performed using a curved hemostat with a gentle bucco-lingual movement.

Animal grouping

The rats were randomly assigned into three groups (GI, GII and GIII) (30 rats each) according to the date of sacrifice 3,7 and 9 days after extraction. The three main groups were further subdivided into three subgroups (10 rats each): ***Control subgroup*** **(Con)** their extraction sockets were left untreated without any material, ***Mg and Zn Bioactive glass subgroups*** their extraction sockets were immediately filled with either Mg or Zn Bioactive glass respectively mixed with BMP-2 (Sigma-Aldrich Co. St. Louis, Missouri, USA) (2 µg/µl in phosphate-buffered saline solution, pH 7.4) to form a paste. The animals were sacrificed by intravenous overdose of pentobarbital sodium. Then the mandibles were carefully dissected and the right side of each mandible was separated.

Histopathological analyses

All the specimens were fixed in 10% calcium formol for 48h, washed and soaked in10% EDTA for decalcification for 4 weeks and then rinsed in distilled water. Specimens were dehydrated in ascending grades of alcohol and embedded in paraffin. Sagital, mesiodistal sectioning of the jaws was carried out. Histological sections were prepared of 5μ thickness. A set of sections were subjected to H&E staining for routine examination and to Masson's trichrome stain for detection of collagen.

Immunohistochemistry

Another set of sections were incubated in hot oven for 2 hours at 56°C, deparaffinized in xylene and rehydrated by ethanol series ending with pure H_2O (Millipore Corporation, Temecula, CA, USA). After 5-minutes washing in phosphate buffer saline (PBS), unmasking of the antigens was carried out using antigen retrieval citrate buffer solution for 10 min in boiling water. Then the sections were placed in a humid chamber and the endogenous tissue peroxidase was blocked with 3% hydrogen peroxide for 5 min. Incubation with bovine serum albumin for 20 min was performed to reduce unwanted non-specific reactions. Without washing, the sections were incubated with the primary antibodies overnight at 4°C. (anti-vascular endothelial growth factor VEGF) (Millipore Corporation, Temecula, CA, USA) with dilutions 1:100. In the next day, after washing in PBS, the sections were incubated with secondary universal antibody (Vectastain Universal Elite ABC- peroxidase kit, Vector Laboratories) and then with the Avidin-Biotin complex (ABC) (Vectastain Universal Elite ABC kit, Vector Laboratories, Burlingame, CA, USA) according to the manufacturer's protocol. The substrate 3,3'-diaminobenzidine (DAB) was applied for the same amount of time on all labeled sections until development of desired brown color. Finally, the sections were counter-stained with Mayer's hematoxylin (Sigma, St. Louis, MO, USA) for 30 sec. to visualize tissue topography. The negative control was obtained by omitting the primary antibody from the protocol outlined above.

Histomorphometric analyses

The data were obtained using Leica Qwin 500 image analyzer computer system (England). The area and the area percentage of newly formed bone trabeculae were measured using an objective lens of magnification 20x (total magnification of 200) in the heamatoxylin and eosin sections. The area percentage of VEGF expression was measured using an objective lens of magnification 40 x, i.e. of a total magnification of 400. Ten fields were measured from each specimen of the study nine subgroups. Using the color detect, areas were masked by a blue binary color. The area percentage was calculated in relation to a standard measuring frame of area 118476.6μm^2. The terminology and units used are those recommended by the Histomorphometry Nomenclature Committee of the American Society for Bone and Mineral Research. [21]

RESULTS

Histological results

Group I (3 days after extraction)

The whole extraction sockets of GI subgroups were presented in (Fig. 2 A,D,G). The socket of control subgroup was filled with dense fibrous connective tissue as well as granulation tissue (Fig. 2 A). Spicules of calcified cartilage, calcified bone matrix and cartilage cells were formed upon the fibrous connective tissue (Fig. 2 B). The newly formed collagen fibers were evidenced (Fig. 2 B,C). Mg subgroup socket was also filled with the dense fibrous connective tissue (Fig. 2 A) but with a relative increase in the amount of hypertrophic cartilage cells (endochondral bone formation) (Fig. 2 E). Calcified bone matrix and calcified cartilage were revealed in this subgroup (Fig. 2 E). The newly formed collagen could be seen in (Fig. 2 E, F). Remnants of the graft material were noticed in Zn subgroup embedded in between the highly cellular and vascular granulation tissue (Fig. 2 H). Woven bone was formed at the base of the socket (Fig. 2 H,I).

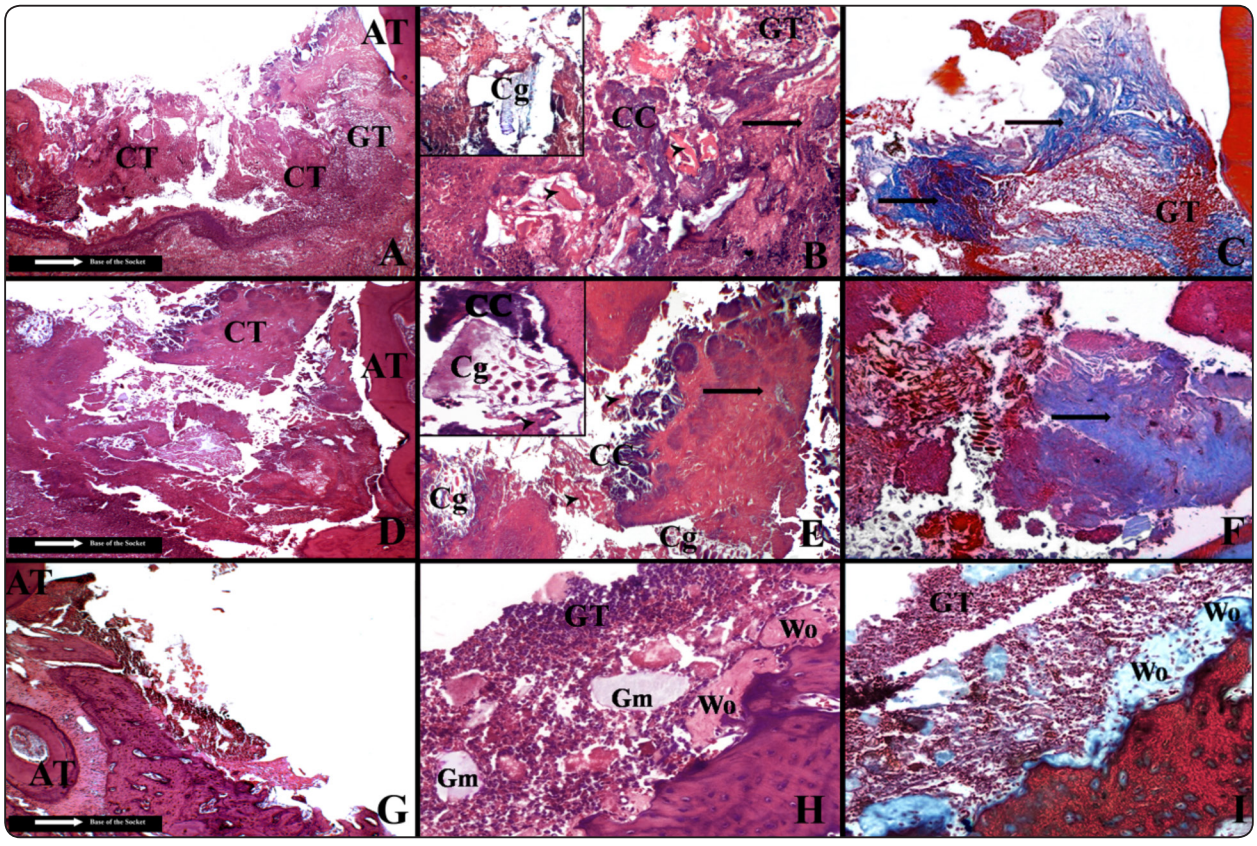

Fig. (2) A photomicrograph of GI (3 days after extraction); Control subgroup [A]: showing the whole socket filled with dense connective tissue (CT) and granulation tissue (GT) as well as the adjacent tooth (AT) . Control subgroup [B]: showing spicules of calcified bone matrix (arrow heads) and calcified cartilage (CC). Inset: showing cartilage cells (Cg). Control subgroup [B,C] showing GT, newly formed collagen fibers (arrows). Mg subgroup [D]: showing the whole socket filled with CT and the adjacent tooth (AT). Mg subgroup [E]: showing CC, calcified bone matrix (arrowheads) and Cg. Mg subgroup [E, F]: showing newly formed collagen fibers (arrows). Inset: showing CC, hypertrophic Cg and calcified bone matrix (arrowheads). Zn subgroup [G]: showing the whole socket with the adjacent tooth (AT). Zn subgroup [H, I] showing: woven bone (Wo), graft material (Gm) within GT. [A, D and G] (H&E stain, Orig. Mag. 40x); [B, E and H] (H&E stain, Orig. Mag. 100x, Insets: Orig. Mag. 200x); [C, F and I] (Masson Trichrom stain, Orig. Mag. 100x)

Group II (7 days after extraction)

The whole extraction sockets of GII subgroups were presented in (Fig. 3 A,D,G). The socket of control subgroup was filled with granulation tissue (Fig. 3 A). Densely packed newly formed collagen fibers as well as spicules of woven bone could be seen at the base of the socket while the lateral wall of the socket was highly remodeled (Fig. 3 B,C). Cartilage cells which denotes endochondral bone formation were revealed in this group (Fig. 3 B). However, the sockets of Mg subgroup and Zn subgroup were partially filled with fibrous connective tissue but the density of the collagen fibers was higher in the Zn subgroup (Fig. 3 D,G). Granulation tissue and newly formed collagen fibers as well as calcified bone matrix were evidenced in both subgroups (Fig. 3 E,H). In addition, hypertrophic cartilage cells, calcified cartilage and woven bone were revealed in the Zn subgroup (Fig. 3 H,I).

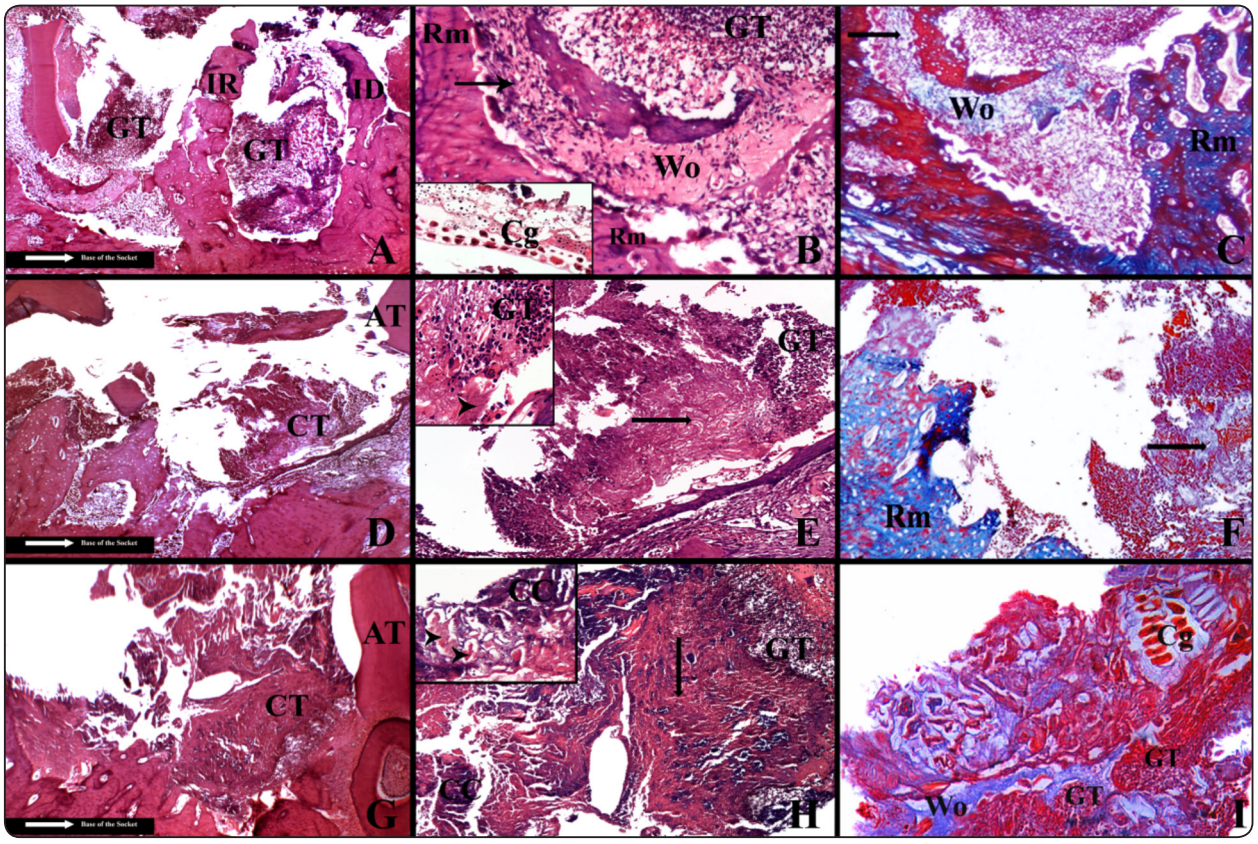

Fig. (3) A photomicrograph of GII (7 days after extraction); Control subgroup [A]: showing the whole socket with the interdental (ID) and interreadicular (IR) septa filled with granulation tissue (GT). Control subgroup [B, C]: showing GT, densely packed collagen fibers (arrows), woven bone (Wo) and remodeled bone (Rm). Inset: cartilage cells (Cg). Mg subgroup [D]: showing the whole socket contained connective tissue (CT) with the adjacent tooth (AT). Mg subgroup [E, F]: showing GT and newly formed collagen fibers (arrows). Inset: calcified bone matrix (arrow head) and GT. Mg subgroup [F]: showing Rm. Zn subgroup [G]: showing the whole socket contained dense CT and the adjacent tooth (AT). Zn subgroup [H]: showing newly formed collagen fibers (arrow), calcified cartilage (CC) and GT. Inset: CC and increased amount of calcified bone matrix (arrowheads); Zn subgroup [I]: showing Wo, GT and Cg. [A, D and G] (H&E stain, Orig. Mag. 40x); [B, E and H] (H&E stain, Orig. Mag. 100x, Insets: Orig. Mag. 200x); [C, F and I] (Masson Trichrom stain, Orig. Mag. 100x)

Group III (9 days after extraction)

The whole extraction sockets of GIII subgroups were presented in (Fig. 4 A,D,G). The socket of control subgroup was filled with dense highly fibrous connective tissue as well as granulation tissue (Fig 4. A,B). Newly formed woven bone upon the highly remodeled old alveolar bone was seen at the lateral wall of the socket (Fig 4. B,C). The socket of Mg subgroup showed large spicule of relatively mature lamellar bone with large number of osteocytes and multiple reversal lines. At the border of these bone spicules there were dense collagen fibers that showed changes in their architecture (Fig 4. E,F). The socket of Zn subgroup was filled with spicules of mature lamellar bone formed upon highly fibrocellular connective tissue (Fig 4.G). The lamellar bone was similar in structure to that formed in Mg subgroup but with smaller amount of osteocytes and with osteon formation. The marrow cavities were large in size some of which were filled with dense fibrous connective tissue that began to arrange in bone at certain areas. There were large numbers of resting and reversal lines in the bone formed in this subgroup (Fig 4. H). The mature lamellar bone with immature bone on its surface could be seen in (Fig 4. I).

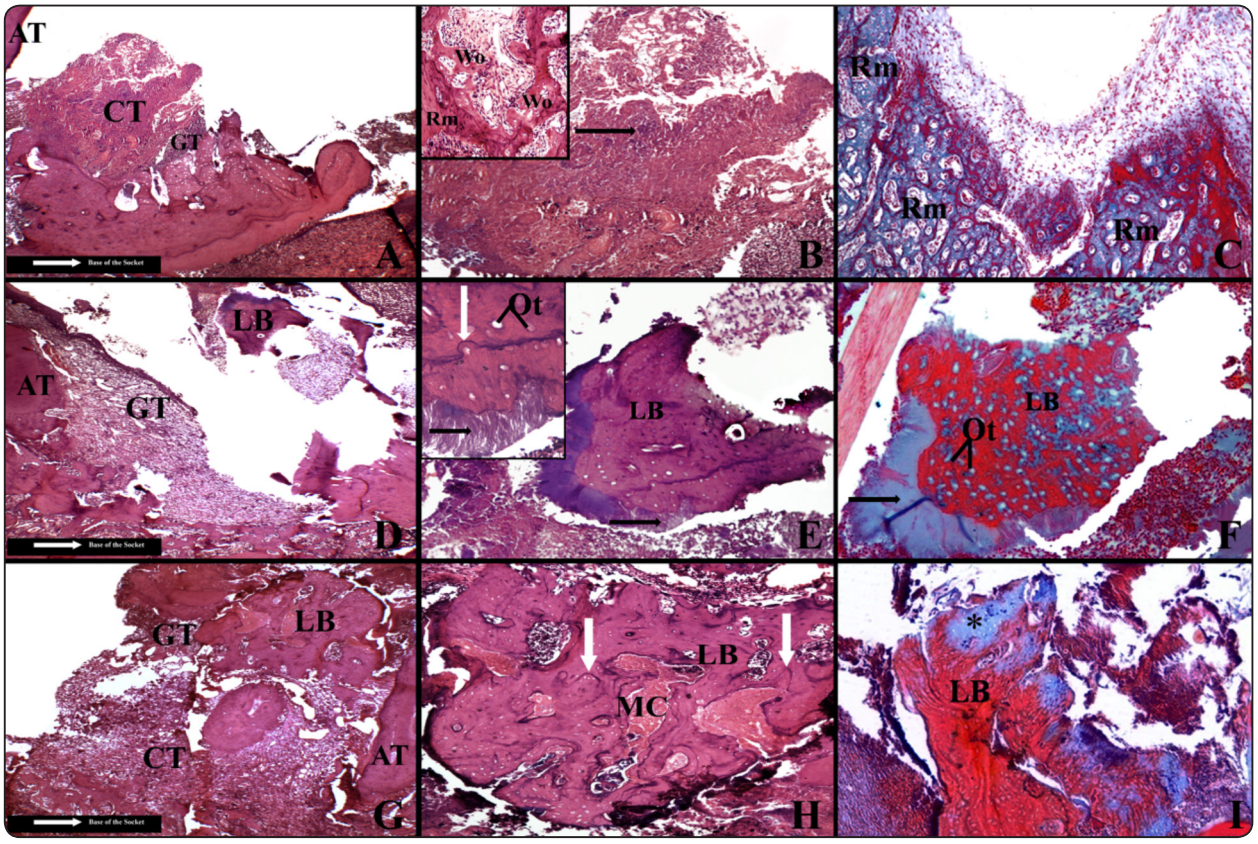

Fig. (4) A photomicrograph of GIII (9 days after extraction); Control subgroup [A]: showing the whole socket filled with dense connective tissue (CT) and granulation tissue (GT) as well as the adjacent tooth (AT). Control subgroup [B]: showing dense collagen fibers (arrow). Inset: showing woven bone (Wo) and remodeled bone (Rm). Control subgroup [C]: showing Rm. Mg subgroup [D]: showing the whole socket contained lamellar bone (LB) and GT with the adjacent tooth (AT). Mg subgroup [E, F]: showing dense newly formed collagen fibers (arrows) with large spicules of relatively mature LB. Inset: osteocytes (Ot) and reversal lines (white arrow). Zn subgroup [G]: showing the whole socket filled with LB, CT and GT as well as the adjacent tooth (AT). Zn subgroup [H]: showing LB with large sized marrow cavities (MC), resting and reversal lines (white arrows). Zn subgroup [I]: showing LB with immature bone (asterisks) [A, D and G] (H&E stain, Orig. Mag. 40x); [B, E and H] (H&E stain, Orig. Mag. 100x, Insets: Orig. Mag. 200x); [C, F and I] (Masson Trichrom stain, Orig. Mag. 100x)

Histomorphometric analyses

The area percentages of the newly formed bone is shown in Table 1. A significant increase in the newly formed bone area percentage has been recorded between the control, Mg and Zn subgroups within GI , GII and GIII where (P<0.001).

Within GI, a significant increase in the neobone area percentage was evident in the sockets of Mg and Zn subgroups as compared to the control ones where (P=0.019 and P<0.001 respectively), while a non significant increase in the neobone area percentage between the sockets of GI (Mg and Zn) subgroups (P= 0.06). Within GII and GIII, there has been an overall high significant increase in the neobone area percentage between Zn, Mg and control subgroups where (P<0.001).

The area percentages of VEGF immunoreaction is shown in Table 2. The histomorphometric analysis for the VEGF expression showed that however there has been a high significant difference in VEGF expression within GI and GIII different subgroups (P=0.002 and P=0.001 respectively), a non significant difference was revealed between GII different subgroups (P=0.267). Within GI, there was a significant increase in Zn and Mg subgroups versus control subgroup (P=0.002 and P=0.015 respectively), while no significant difference between Zn and Mg subgroups (P=0.2) has been recorded.

Within GII, there was a non significant difference in VEGF expression between Zn subgroup versus Mg and control subgroups (P=0.47, P=0.149 respectively) as well as between Mg subgroup versus control subgroup (P=0.24). On the other hand within GIII, there has been a significant increase in VEGF expression in Zn subgroup versus Mg and control subgroups (P=0.02, P=0.001 respectively) as well as between Mg subgroup versus control subgroup (P=0.04).

TABLE (1) The area percentages of the newly formed bone in the sockets of GI, GII and GIII (control, Mg and Zn) subgroups.

	GI 3 days after extraction	GII 7 days after extraction	GIII 9 days after extraction
Control subgroup	30.987 ± 8.223	60.416 ± 7.188	70.722 ± 3.921
Mg subgroup	43.659 [a] ± 13.153	104.432 [a] ± 6.954	123.317 [a] ±3.277
Zn subgroup	52.249 [a] ± 3.134	130.609 [a,b] ± 3.665	175.470 [a,b] ± 6.099
p value	< 0.001*	< 0.001*	< 0.001*

Data presented as mean±SD; * statistically significant difference; [a] statistically significant with the control subgroup; [b] statistically significant with the Mg subgroup

TABLE (2) The area percentages of vascular endothelial growth factor immunoreaction in the sockets of GI, GII and GIII (control, Mg and Zn) subgroups.

	GI 3 days after extraction	GII 7 days after extraction	GIII 9 days after extraction
Control subgroup	3.076 ± 0.256	4.818 ± 0.768	5.579 ± 0.728
Mg subgroup	4.215 [a] ± 1.309	5.276 ± 0.922	6.66 [a] ± 1.3392
Zn subgroup	4.968 [a] ± 1.235	5.7366 ± 1.7666	9.415 [a,b] ± 3.047
p value	0.002*	0.267	0.001*

Data presented as mean±SD; * statistically significant difference; [a] statistically significant with the control subgroup; [b] statistically significant with the Mg subgroup

DISCUSSION

Impaired wound healing is one of the major problems facing diabetic patients. Following tooth loss, extraction site reconstruction is essential for alveolar ridge preservation. In an attempt to improve the healing and bone regeneration in extraction sockets of diabetic patients, numerous biocompatible regenerative materials have been used immediately following tooth extraction to fill the socket. This study compared between the effects of magnesium versus zinc enriched nano-sized bioactive glass mixed with BMP-2 as a scaffold material when applied to extraction sockets in streptozotocin induced diabetic rats.

In the current work the area percentage of the newly formed bone in Mg and Zn bioactive glass subgroups was higher than that in the diabetic control subgroup. It is well known that diabetes impairs both soft and hard tissue wound healing. Although, Type 1 but not Type 2 diabetes is associated with decreased bone mineral density, both are associated with an increased likelihood of bone fracture.[22] Several contributing factors have been reported, such as prolonged expression of cytokines and chemokines; destruction of matrix that is associated with an imbalance between matrix lytic enzymes and their inhibitors [23]; as well as defects in the reparative capacity because of diminished production of growth and angiogenic factors, decreased proliferation and increased apoptosis. [24]

Furthermore, diabetes impairs fracture healing of bone, including the mandible, hip and long bones.[25, 26] Clinical studies have reported delayed union or increased healing time in diabetic subjects compared with matched controls.[27-29] Long-bone fractures of streptozotocin-induced diabetic animals also exhibit changes consistent with impaired healing, including smaller calluses with decreased bone and reduced mechanical strength compared with those of controls. [30, 31]

In the present study, both Mg and Zn bioactive glass subgroups induced the formation of more neobone than the control diabetic subgroups at different study intervals. Bioactive glass is a biocompatible, osteoconductive material that forms a strong bond with living tissue via the formation of a hydroxyapatite layer on their surface [32] and has been used to repair hard tissues in a variety of craniofacial, maxillofacial and periodontal

applications.[33,34] Moreover, nanotechnology and composite materials provide new ways to improve the strength and toughness of bioactive ceramics. Bioactive nanoglass exhibits great potential for bone repair due to better mechanical and biological properties. [35]

Bone regeneration and socket healing were demonstrated in all present investigation subgroups; control, Mg and Zn bioactive glass mixed with BMP-2. In the control sites, healing occurred at a comparatively slower rate than in the BMP-2 sites. BMPs in general induce a complex cascade of chemotaxis, proliferation and cellular differentiation that closely resembles the normal process of embryonic bone formation, including both intramembranous and endochondral bone. [36]

The reported delayed bone healing in the control subgroups in the herein study, could be referred to diabetes as diabetes is associated with defects in the reparative capacity due to diminished production of growth and angiogenic factors. [37-39] Furthermore, the cartilage cells detected in both GI and GII in the present study, could be also attributed to diabetes which is associated with diminished vasculature that induce chondrogenesis rather than osteogenesis.

In the present work, the endochondral ossification observed in GI Mg subgroup and GII Mg and Zn subgroups was similarly reported by Ting et al. [40] and King et al.[41] . King et al.[41] referred the endochondral bone formation in rat mandibular defects to the low concentrations of applied BMP-2 that may induce chondrogenesis. Other studies that demonstrated direct osteogenesis, concluded that differences in culture system (*in vitro*) or environment of graft sites (*in vivo*) may be responsible for cartilage induction or non-induction.[42,43] On the other hand Ting et al,[40] demonstrated cartilage phenotypic expression α1(II) and α1(IX) mRNAs sequentially during the intramembranous bone formation in extraction rat sockets. They concluded that the expression of collagen II and IX may represent an early phenotypic feature of osteoblastic differentiation.

In the ongoing study, the area percentage of newly formed bone was significantly higher in GII and GIII Zn subgroups than in the same Mg subgroups.

These results could be explained on the basis that Zn-substituted bioactive glass creates a template for osteoblastic proliferation and differentiation by the interaction between the Zn and inorganic phosphate at the surface of the bioactive glass. So it can improve the ability of glass to bond with bone. [44] It has been proved that, addition of Zn has a synergistic effect on cell attachment which also maintains the pH within the physiological limit by forming zinc hydroxide in the solution. Furthermore, Aina et al. [45] and Haimi et al. [46] reported that limited amounts of Zn in the bioactive glass system stimulates early cell proliferation and promotes differentiation as assessed by their *in vitro* biocompatibility experimentation.

Many authors reported that bioactive glass stimulated the secretion of angiogenic growth factors in fibroblasts [47-50], the proliferation of endothelial cells [47, 51-53] and the formation of endothelial tubules[47, 51]. The VEGF results of the present study supported that, as both Mg and Zn bioactive glass subgroups demonstrated enhanced neovascularization. However the results of the Zn subgroups were more promising.

The significant increase in VEGF expression in the Zn bioactive glass subgroup in GI and GIII in the present study could be attributed to the microstructure of pores provided by this material. Rattanachan et al. [54] demonstrated that Zn enhanced bioglass showed interconnected macropores in the range of 300-500 μm and the average pore size increased with increasing the zinc additions. They added that by controlling the zinc concentrations the size of macropores can be tailored.[54]

Furthermore it has been reported that pores in the range of 150–800 μm allow the ingrowths of bone tissue and blood vessels while pores in the range of 10–100 μm are beneficial for the growth of blood capillaries, exchange of nutrients and excretion of waste products. Pores in the range of nanoscale provide larger specific surface area and more active targets, which is good for the formation of apatite and the attachment of protein or osteoblast. [55]

In the current study, the role of the Mg enriched scaffold was relatively of little value in comparison to Zn enriched scaffold regarding the rate and the amount of newly formed bone and angiogenesis. On the other hand the Mg enriched bioactive glass showed an enhanced bone regenerative capacity and angiogenesis as compared to the control diabetic group. It is known that magnesium is involved in over 300 chemical reactions in the body, it activates phagocytosis and regulates active calcium transport. Circumstantial evidence exists that MgO improves the early mineralization stages and contributes to an intimate contact with living tissue. [56-58]

Furthermore, the release of Mg ions upon degradation could enhance the viability of pre-osteoblasts, cell adhesion and also could stimulate bone growth and bone healing. [59]

Authors reported that the in situ release of magnesium ions is able to stimulate local bone formation and bone healing by enhancing the osteoblastic and osteoclastic activities.[60,61] However, the amount of Mg ions released is critical for bone formation. [62] Too much ions released would lead to bone loss. [63]

The longest term in the present study was 9 days. However, it is well documented that laboratory animals regenerate oral tissues much faster than humans do and that during nursing 42.4 rat days equals one human year, while during adolescence 10.5 rat days equals one human year, with an average 16.7 days [64,65], literatures studied extraction wound healing in rats till 3-4 weeks [66,67]. On the otherhand, Yoneda et al.[68], reported that after extraction of maxillary first molar and treating it with coenzyme Q10 the clot was replaced with granulation tissue at 3 days and at 8 days osteoid and woven bone were observed in the socket, indicative of the callus stage of wound healing.

The overall results of the present research, clarify that although the Mg enriched bioactive glass subgroups were lagging behind the Zn enriched bioactive glass ones, both were beneficial in enhancing the wound healing capacity in extraction sockets of diabetic rats regarding the amount of newly formed bone and angiogenesis.

REFERENCES

1. Mathieu D, Linke JC and Wattel F. Non-healing wounds. In: Handbook on hyperbaric medicine, Mathieu D (ed). Netherlands: Springer, 2006: 401-428.
2. Woo K, Ayello EA and Sibbald RG. The edge effect: current therapeutic options to advance the wound edge. Adv Skin Wound Care. 2007; 20(2): 99-117.
3. Huijberts MS, Schaper NC and Schalkwijk CG. Advanced glycation end products and diabetic foot disease. Diabetes Metab Res Rev. 2008; 24 Suppl 1:S19-24.
4. Gary Sibbald R and Woo KY. The biology of chronic foot ulcers in persons with diabetes. Diabetes Metab Res Rev. 2008;24 Suppl 1:S25-30.
5. Gallagher KA, Liu ZJ, Xiao M. et al. Diabetic impairments in NO-mediated endothelial progenitor cell mobilization and homing are reversed by hyperoxia and SDF-1 alpha. J Clin Invest. 2007;117(5):1249-1259.
6. Quattrini C, Jeziorska M, Boulton AJ and Malik RA. Reduced vascular endothelial growth factor expression and intra-epidermal nerve fiber loss in human diabetic neuropathy. Diabetes Care. 2008; 31(1):140-145.
7. Sanada JT, Rodrigues JG, Canova GC. et al. Histologic, radiographic and imunoglobuline profile analysis after implantation blocks of demineralized bovine cancellous bone graft in muscle of rats. J Appl Oral Sci. 2003;11(3):209-215.
8. Christensen GJ. Ridge preservation: Why not? J Am Dent Assoc. 1996;127(5):669-670.
9. Camargo PM, Lekovic V, Weinlaender M. et al. Influence of bioactive glass on changes in alveolar process dimensions after exodontia. Oral Surg Oral Med Oral Pathol Oral Radiol Endod. 2000;90(5):581-586.

10. Perri de Carvalho PS, Bassi APF and Pereira LAVD. Review and proposal of nomenclature for biomaterials. Implant News 2004;1:255-260

11. Moore WR, Graves SE and Bain GI. Synthetic bone graft substitutes. ANZ J Surg. 2001;71(6):354-361.

12. Lim BS, Jeon JY, Park CJ, Im JJ, Hwang KG and Shim KS. The BMPs expression and histomorphometric study of β-TCP/rhBMP-2 Grafting on the rabbit cranial bone defects. J Kor Oral Maxillofac Surg. 2008; 34(1): 49-58.

13. Wu C and Chang J. Mesoporous bioactive glasses: structure characteristics, drug/growth factor delivery and bone regeneration application. Interface Focus. 2012; 2(3):292-306.

14. Chasapis CT, Loutsidou AC, Spiliopoulou CA and Stefanidou ME. Zinc and human health: an update. Arch Toxicol. 2012;86(4):521-534.

15. Fraker PJ and King LE. Reprogramming of the immune system during zinc deficiency. Annu Rev Nutr. 2004; 24: 277-298.

16. Bao B, Prasad AS, Beck FW. et.al. Zinc decreases C-reactive protein, lipid peroxidation, and inflammatory cytokines in elderly subjects: a potential implication of zinc as an atheroprotective agent. Am J Clin Nutr. 2010;91(6):1634-1641.

17. Altura BM, Altura BT, Carella A and Turlapaty PD. Ca^{2+} coupling in vascular smooth muscle: Mg^{2+} and buffer effects on contractility and membrane Ca^{2+} movements. Can J Physiol Pharmacol. 1982; 60(4):459–482.

18. D'Angelo EK, Singer HA and Rembold CM. Magnesium relaxes arterial smooth muscle by decreasing intracellular Ca^{2+} without changing intracellular Mg^{2+}. J Clin Invest. 1992;89(6):1988-1994

19. Nadler JL, Goodson S and Rude RK. Evidence that prostacyclin mediates the vascular action of magnesium in humans. Hypertension. 1987;9(4):379-383.

20. Landau R, Scott JA and Smiley RM. Magnesium-induced vasodilation in the dorsal hand vein. BJOG. 2004; 111(5):446-451.

21. Parfitt AM, Drazner MK, Glorieux FH. et al. Bone histomorphometry: standardization of nomenclature, symbols, and units. J Bone Miner Res. 1987;2(6):595-610.

22. Adami S. Bone health in diabetes: considerations for clinical management. Curr Med Res Opin. 2009; 25(5): 1057-1072.

23. Lobmann R, Ambrosch A, Schultz G, Waldmann K, Schiweck S and Lehnert H. Expression of matrix-metalloproteinases and their inhibitors in the wounds of diabetic and non-diabetic patients. Diabetologia. 2002;45(7):1011-1016.

24. Graves DT and Kayal RA. Diabetic complications and dysregulated innate immunity. Front Biosci. 2008;1;13:1227-1239.

25. Ohnishi T, Bandow K, Kakimoto K, Machigashira M, Matsuyama T and Matsuguchi T. Oxidative stress causes alveolar bone loss in metabolic syndrome model mice with type 2 diabetes. J Periodontal Res. 2009;44(1):43-51.

26. Senel FC, Jessen GS, Melo MD and Obeid G. Infection following treatment of mandible fractures: the role of immunosuppression and polysubstance abuse. Oral Surg Oral Med Oral Pathol Oral Radiol Endod. 2007; 103(1):38-42.

27. Cozen L. Does diabetes delay fracture healing?. Clin Orthop Relat Res. 1972;82:134-140.

28. Loder, R. The influence of diabetes mellitus on the healing of closed fractures. Clin Orthop Relat Res. 1988; 232:210-216.

29. Herskind AM, Christensen K, Norgaard-Andersen K and Andersen JF. Diabetes mellitus and healing of closed fractures. Diabetes Metab. 1992;18(1):63-64.

30. Gooch HL, Hale JE, Fujioka H, Balian G and Hurwitz SR. Alterations of cartilage and collagen expression during fracture healing in experimental diabetes. Connect Tissue Res. 2000;41(2):81-91.

31. Macey LR, Kana SM, Jingushi S, Terek RM, Borretos J and Bolander ME. Defects of early fracture-healing in experimental diabetes. J Bone Joint Surg Am. 1989;71(5): 722-733.

32. Hench LL, Splinter RJ, Allen WC and Greenlee TK. Bonding mechanisms at the interface of ceramic prosthetic materials. J Biomed Mat Res. 1971; 5 (6): 117-141.

33. Mardare CC, Mardare AI, Fernandes JRF. et al. Deposition of bioactive glass-ceramic thin-films by RF magnetron sputtering. J Eur Ceram Soc. 2003, 23:1027–1030.

34. Ghosh SK, Nandi SK, Kundu B. et al. In vivo response of porous hydroxyapatite and β-tricalcium phosphate prepared by aqueous solution combustion method and comparison with bioglass scaffolds. J Biomed Mater Res B Appl Biomater. 2008;86(1):217-227.

35. Du RL, Chang J, Ni SY, Zhai WY and Wang JY. Characterization and in vitro Bioactivity of Zinc-containing Bioactive Glass and Glass-ceramics . J Biomater Appl. 2006; 20 (4): 341-360.

36. Reddi AH and Huggins C. Biochemical sequences in the transformation of normal fibroblasts in adolescent rats. Proc Natl Acad Sci USA. 1972;69 (6):1601–1605.

37. Wetzler C, Kampfer H, Stallmeyer B, Pfeilschifter J and Frank S. Large and sustained induction of chemokines during impaired wound healing in the genetically diabetic mouse prolonged persistence of neutrophils and macrophages during the late phase of repair. J Invest Dermatol. 2000; 115(2): 245-253.

38. Lobmann R, Ambrosch A, Schultz G, Waldmann K, Schiweck S and Lehnert H. Expression of matrix-metalloproteinases and their inhibitors in the wounds of diabetic and non-diabetic patients. Diabetologia. 2002; 45 (7): 1011–1016.

39. Graves DT and Kayal RA. Diabetic complications and dysregulated innate immunity. Front Biosci. 2008; 13: 1227–1239.

40. Ting K, Petropulos LA, Iwatsu M and Nishimura I. Altered cartilage phenotype expressed during intramembranous bone formation. J Bone Miner Res. 1993;8 (11):1377–87.

41. King GN, King N, Cruchley AT, Wozney JM and Hughes FJ. Recombinant human bone morphogenetic protein-2 promotes wound healing in rat periodontal fenestration defects. J Dent Res. 1997;76 (8):1460–1470.

42. Iwasaki M, Nakahara H, Nakase T, et al. Bone morphogenetic protein-2 stimulates osteogenesis but does not affect chondrogenesis in osteochondrogenic differentiation of periosteoum-derived cells. J Bone Miner Res. 1994;9 (8): 1195–1204.

43. Rosen V and Thies RS. The BMP proteins in bone formation and repair. Trends Genet. 1992;8 (3):97–102.

44. Aina V, Perardi A, Bergandi L. et al. Cytotoxicity of zinc-containing bioactive glasses in contact with human osteoblasts. Chem Biol Interact. 2007; 167 (3): 207–218.

45. Aina V, Malavasi G, FiorioPla A, Munaron L and Morterra C. Zinc-containing bioactive glasses: Surface reactivity and behaviour towards endothelial cells. Acta Biomater. 2009; 5(4): 1211-1222.

46. Haimi S, Gorianc G, Moimas L. et al. Characterization of zinc-releasing three-dimensional bioactive glass scaffolds and their effect on human adipose stem cell proliferation and osteogenic differentiation. Acta Biomater. 2009; 5 (8): 3122-3131.

47. Day RM. Bioactive glass stimulates the secretion of angiogenic growth factors and angiogenesis in vitro. Tissue Eng. 2005; 11 (5-6): 768-677.

48. Keshaw H, Georgiou G, Blaker JJ, Forbes A, Knowles JC and Day RM. Assessment of polymer/bioactive glass-composite microporous spheres for tissue regeneration applications. Tissue Eng. Part A. 2009;15 (7): 1451-1461.

49. Day RM, Boccaccini AR, Shurey S. et al. Assessment of polyglycolic acid mesh and bioactive glass for soft-tissue engineering scaffolds. Biomater. 2004; 25: 5857-5866.

50. Moosvi SR and Day RM. Bioactive glass modulation of intestinal epithelial cell restitution. Acta Biomater. 2009;5(1):76-83.

51. Leu A and Leach JK. Proangiogenic potential of a collagen/bioactive glass substrate. Pharm Res. 2008; 25(5): 1222-1229.

52. Keshaw H, Forbes A and Day RM. Release of angiogenic growth factors from cells encapsulated in alginate beads with bioactive glass. Biomaterials. 2005; 26 (9): 4171-4179.

53. Leach JK, Kaigler D, Wang Z, Krebsbach PH and Mooney DJ. Coating of VEGF-releasing scaffolds with bioactive glass for angiogenesis and bone regeneration. Biomaterials. 2006; 27 (17): 3249-3255.

54. Rattanachan ST, Srakaew N, Pethnin R and Suppakarn N. Effect of Zn Addition on Sol-Gel Derived Apatite/Wollastonite Glass-Ceramics Scaffolds. J Metal Mater Miner. 2012; 22 (2): 61-65.

55. Lü R, Zhou W, Shi K. et al. Alumina decorated TiO_2 nanotubes with ordered mesoporous walls as high sensitivity of NO gas sensors at room temperature. Nanoscale. 2013;5 (18):8569–8576.

56. Spasov AA., Fomichev EV, Guseva TN, Mazanova LS and Shchava S N. Efficiency of magnesium-containing preparation polykatan in therapy of purulent wounds. Bulletin of experimental biology and medicine. Bull Exp Biol Med. 2001;131(2):132-135.

57. Sojka JE and Weaver CM. The role of nutrition in osteoporosis. Nutr Rev. 1995; 53(3): 71-74.

58. Oliveira JM, Correia RN, Fernandes MH and Rocha J. Influence of the CaO/MgO ratio on the structure of phase-separated glasses: a solid state Si-29and P-31 MAS NMR study. J Non-Cryst. 2000; 265(3): 221-229.

59. Wong HM, Chu PK, Leung FK, Cheung KM, Luk KD and Yeung KW. Engineered polycaprolactone–magnesium hybrid biodegradable porous scaffold for bone tissue engineering. Prog Nat Sci: Mater Int. 2014; 24(5): 561-567.

60. Wong HM, Wu S, Chu PK. et. al. Low-modulus Mg/PCL hybrid bone substitute for osteoporotic fracture fixation. Biomaterials. 2013; 34(29): 7016-7032.

61. Boanini E, Gazzano M and Bigi A. Ionic substitutions in calcium phosphates synthesized at low temperature. Acta Biomater. 2010; 6 (6):1882–1894.

62. Park JW, Kim YJ, Jang JH and Song H. Osteoblast response to magnesium ion-incorporated nanoporous titanium oxide surfaces. Clin Oral Implants Res. 2010; 21(11): 1278–1287.

63. Serre CM, Papillard M, Chavassieux P, Voegel JC and Boivin G. Influence of magnesium substitution on a collagen–apatite biomaterial on the production of a calcifying matrix by human osteoblasts. J Biomed Mater Res. 1998; 42(4): 626–633.

64. Quinn R. Comparing rat's to human's age: How old is my rat in people years?. Nutrition. 2005;21:775–777.

65. Sengupta PA. Scientific Review of Age Determination for a Laboratory Rat: How old is it in comparison with Human age? Biomed Int. 2012;2:81–89.

66. Kuroshima S, Kovacic BL, Kozloff KM, McCauley LK and Yamashita J. Intra-oral PTH administration promotes tooth extraction socket healing. J Dent Res. 2013; 92: 553–559.

67. Mendes RM, Silva GA, Lima MF. et al. Sodium hyaluronate accelerates the healing process in tooth sockets of rats. Arch Oral Biol. 2008; 53: 1155–1162.

68. Yoneda T, Tomofuji T, Kawabata Y. et al. Application of coenzyme Q10 for accelerating soft tissue wound healing after tooth extraction in rats. Nutrient. 2014; 6(12): 5756-5769.